



LJMU Research Online

Armada Bras, AM, Antunes, A, Laborel-Preneon, A, Ralegaonkar, R, Shaw, A, Riley, ML and Fariae, P

Optimisation of bio-based building materials using image analysis method

<http://researchonline.ljmu.ac.uk/id/eprint/11022/>

Article

Citation (please note it is advisable to refer to the publisher's version if you intend to cite from this work)

Armada Bras, AM, Antunes, A, Laborel-Preneon, A, Ralegaonkar, R, Shaw, A, Riley, ML and Fariae, P (2019) Optimisation of bio-based building materials using image analysis method. Construction and Building Materials, 223. pp. 544-553. ISSN 0950-0618

LJMU has developed **LJMU Research Online** for users to access the research output of the University more effectively. Copyright © and Moral Rights for the papers on this site are retained by the individual authors and/or other copyright owners. Users may download and/or print one copy of any article(s) in LJMU Research Online to facilitate their private study or for non-commercial research. You may not engage in further distribution of the material or use it for any profit-making activities or any commercial gain.

The version presented here may differ from the published version or from the version of the record. Please see the repository URL above for details on accessing the published version and note that access may require a subscription.

For more information please contact researchonline@ljmu.ac.uk

<http://researchonline.ljmu.ac.uk/>

Optimisation of bio-based building materials using image analysis method

Ana Brás¹, Ana Antunes², Aurélie Laborel-Préneron³, Rahul Ralegaonkar⁴, Andy Shaw¹, Mike Riley¹; Paulina Faria⁵

¹ Built Environment and Sustainable Technologies (BEST) Research Institute, Liverpool John Moores University, United Kingdom

² Civil Engineering Department, FCT, NOVA University of Lisbon, Portugal

³ LMDC, Université de Toulouse, UPS, INSA, Toulouse, France

⁴ Department of Civil Engineering at VNIT, Nagpur, India

⁵ CERIS and Civil Engineering Department, FCT, NOVA University of Lisbon, Portugal

Corresponding author: Ana Bras, a.m.armadabras@ljmu.ac.uk

Abstract

Wetting of bio-based mortars — the affinity of the biofibres and earth to the water — can have a strong impact on the flow, but the microscale physics and macroscopic consequences remain poorly understood, not helping in the material optimisation. This research analyses the influence of casting on biofibres dispersion in bio-based insulation materials at the macro-level and evaluate changes on hygrothermal behaviour if fibres and casting change. Earth-based blocks reinforced with 3% weight content of barley straw, hemp shiv and rice husk fibres were produced with 5 and 4 cm thickness using two casting methods. The 5 cm blocks were unstabilised and compacted; the 4 cm blocks were moulded and stabilised with gypsum and air lime. The approach is to implement a developed method of image analysis to elucidate the inherently 2D pore-scale mechanisms and help explain the striking macroscopic displacement patterns that emerge. The results indicate that production variables have a significant directionally dependent impact on the physical properties of cast bio-based materials. This means that the Image analysis can be used for quality control towards the optimisation of the bio-composites. Thermal conductivity and ultra sound velocity are affected by fibres distribution inside bio-based materials. The shape of ultra sound distribution from direct and indirect methods enhance the anisotropy of the bio-based materials with different composition and casting methods.

Keywords: Earth block; Image analysis; Natural fibre; Casting; Energy efficiency; Bio-based composite.

1. Introduction

1.1. Bio-based building materials

Bio-based materials are a promising solution to optimise buildings thermal performance and environmental sustainability. They are known for having low energy requirements and low costs. They improve indoors acoustic and thermal conditions and, on a global scale, this type of materials reduces the carbon emissions once they are mainly composed by natural and available products with reduced environmental impact (Asdrubali et al. 2016).

Being a natural, available and with low environmental impact material, earth is an excellent raw material for bio-based building products. Besides the ecological advantages, earth has high hygroscopic behaviour allowing it to regulate the indoor climate (Minke 2006, McGregor et al. 2014, Binici et al. 2005). The main weaknesses of earth are its poor tensile and flexural strength, ductility and water resistance (Aymerich et al. 2012). Additives are typically added to earth composites, like natural fibres that minimise some of the negative effects and improve some properties (Minke 2006, Laborel-Préneron et al. 2016).

The addition of natural fibres in earth composites has extended to several earth construction techniques like monolithic cob walls, masonry earth blocks such as adobe, compressed earth blocks (CEB) and extruded earth blocks (EEB), and earth mortars. Despite the fibre addition, these techniques have differences concerning their production process, mixture, curing and stabilisation. Adobe are produced with the earth mix in plastic state, generally moulded in wood frames, demoulded still in the fresh state and dried in the air (Laborel-Préneron et al. 2016). They can be stabilised with binders where the most common is air lime. CEB are very similar to adobe with the difference that the earth mix is only humid and the blocks are compressed manually or mechanically. The earth blocks can be extruded (EEB) and in this case the water content of the mix is higher (similar to adobe) to facilitate extrusion (Laborel-Préneron et al. 2016). The stabilisation of CEB with addition of binders is very common, like air lime, hydraulic lime (Gullu & Khudir 2014, Binici et al. 2005), cement (Rim et al. 1999, Obonyo

1 et al. 2010, Binici et al. 2007) or even organic stabilisers as beetroot (Achenza & Fenu 2007) and other organic polymers
2 (Ikeagwuani, et al 2019). With gypsum is not so common, although hemihydrated gypsum is produced with a very low firing
3 temperature (120-180°C) in comparison with air lime (around 900°C) that in turn is produced at a temperature about 30% lower
4 than cement. Earth mortars can be used for applications as filling for wattle and daub wood structure, as layering mortar for
5 masonry or as plaster. Plasters are defined as mixtures composed by clay and sand, water and sometimes plant aggregates
6 (Laborel-Préneron et al. 2016, Antunes et al. 2017, Lima and Faria, 2016), which can contain stabilisers, namely when used
7 as renders (Faria et al. 2016).

8 Through the years several authors studied the addition of natural fibres to earth composites, studying the influence of these
9 natural aggregates on the mechanical, thermal and physical properties (Bouguerra et al. 1998; Bouguerra et al. 1998, Khedari
10 et al. 2005, Ledhem et al. 2000, Obonyo et al. 2010; Faria P, Brás A (2017); Liuzzi S et al. 2018; Brouard et al 2018). Those
11 materials properties can present an anisotropic arrangement, as it was found in bio-aggregate concretes through observations
12 of some physical properties (Williams et al, 2016) .

13 An increase of 30% thermal conductivity in the perpendicular direction to casting was found for cast-compressed hemp-lime
14 specimens (Nguyen et al. 2010). Other work has reported similar findings for cast-tamped material (Dinh et al. 2015) and
15 sprayed material (Pierre et al. 2014). In all cases, the observations were attributed to the internal structure, in which the
16 stratified planes are opposing the transverse heat transfer.

17 The properties of fibre, such as its length, width and strength, as well as its content, can have a strong influence on the
18 compressive and flexural strength of the composites, once the fibres occupies volume among the earthen matrix. Millogo et
19 al. (Millogo et al. 2014) verified that the addition of hibiscus cannabius fibres to earth blocks increased both compressive and
20 tensile flexural strength. The same trend was observed by (Achenza & Fenu 2007, Galán-Marín et al. 2010, Taallah et al.
21 2014). Lima & Faria (Lima and Faria, 2016) observed that the addition of fibres to earth plasters could have different results.
22 While oat straw decreased the mechanical resistance, typha wool increased it, suggesting that the influence of the natural
23 fibres on these properties is connected to the fibre characteristics.

24 When talking about the thermal conductivity some researchers (Rim et al.1999, Millogo et al. 2014, Binici et al. 2007,
25 Laborel-Préneron et al. 2018) concluded that the addition of natural fibres has a positive effect on the thermal conductivity,
26 by decreasing its value.

27 The previous research works demonstrate that the thermal and mechanical properties of bio-aggregate composites are
28 anisotropic, as a result of an orientated internal arrangement of fibres. Therefore, the internal structure of earthen-fibres
29 composite materials seems to be crucial in the optimisation of their physical properties and this has been the focus of the study
30 presented here.

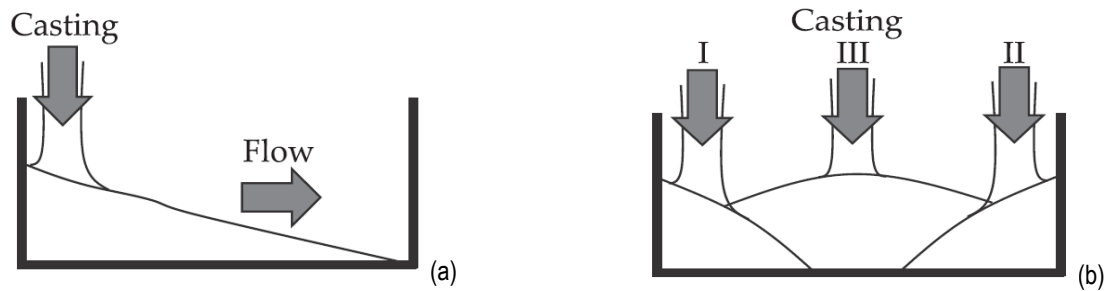
31

32 1.2. 2D image analysis methods

33 Several studies were developed in the field of 2D analysis of composites, namely on the characterisation of asphalt hot mixes,
34 where the behaviour is influenced by its aggregates mechanical and geometrical properties. Since these aggregates play a
35 very important role in the pavement stability and resistance, their characterisation should pass by the determination of length,
36 shape, orientation and texture (Bessa et al. 2012).

37 Bessa et al. (2012) studied the characterisation of three types of aggregates (granitic, construction and demolition waste and
38 steel slag) with the use of digital image processing software that involves the digitalization of a planar image of the composites.
39 This image analysis requires some steps: the transformation of the real image on a digital one, the enhancement of the image
40 so that the particles can be more evidenced, correction of imperfections and finally the segmentation.

41 Yoo et al. (2016) studied the influence of the casting method on ultra high-performance fibre reinforced concrete. Figure 1
42 presents the main conclusions.



1

Figure 1 – (a) Casting procedure that provides the best fibre orientation - higher number of fibres per unit area and concrete reaching the highest flexural strength; (b) procedure leading to lower number of fibres per unit area - insufficient time to align the fibres which leads to poor fibre orientation (Yoo et al. 2016).

1 Generally, during casting a unidirectional compacting force is applied to the wet material by tamping or deliberate compaction.
 2 As biofibres are often elongated in form, this compacting force is considered to have significant influence on their arrangement
 3 and the elongated particles tends towards stratified planes that are perpendicular to compacting force.

4 The assessment of the internal structure of bio-aggregate concretes by image analysis may be a suitable method for the
 5 assessment of these materials. Software like ImageTool, Abaqus 2008, Image J and the Digital Image Analysis System were
 6 referenced by Bessa et al. (2012) as commonly used for this type of analysis, being the last two the ones used by the authors.
 7 Also, Sebaibi et al. (2014) used the ImageJ software on a cement matrix reinforced with polyester and glass fibres to analyse
 8 the number of fibres, their position and orientation.

9 Yoo et al. (2016) introduced a different approach to the image analysis with the use of Photoshop to study the influence of
 10 fibre orientation on the flexural behaviour of ultra high-performance fibre reinforced concrete: firstly, the composite was cut
 11 using a diamond blade; then a picture of the surface was taken with a high-resolution camera that is called RGB image; the
 12 image was passed to a binary image in order to have a segmentation between the fibres and the matrix; finally, with
 13 mathematical expressions, the length and orientation of the fibres were measured.

14 The principal issue of these digital image processes is the segmentation of the images, which is a process that separates
 15 shapes, sorting out particles from the respectively matrix, like the granitic aggregate from the matrix in Bessa et al. (2012) or
 16 the glass fibre from the cementitious matrix from Sebaibi et al. (2012).

17 2. Materials Characterisation and test procedures

18 2.1 Materials

19 2.1.1 Fibres used for the bio-based blocks production

20 The objective was to produce bio-based blocks with rice husk, hemp shiv and barley straw fibres, with 20x20 cm² with 5 cm
 21 and 4 cm thickness, using different casting methods, and then compare their physical properties and the influence of those
 22 methods.

23 For the time being there is no standardised method for plant aggregates characterisation. Laborel-Préneron et al. (2017a)
 24 characterised barley straw, hemp shiv and corn cob based on the work of RILEM TC 236-BBM (Amziane et al. 2017). Barley
 25 Straw (S) is the part of cereal's stem rejected during the harvest. Hemp shiv (H) is the by-product of the hemp defibration
 26 process and corresponds to the lignin-rich part of the stem. Based on the method used and adopting it for rice husk (RH)
 27 characterisation, this natural aggregate was characterised regarding the bulk density, thermal conductivity and water
 28 absorption. Table 1 presents the bulk density values and water absorption for barley straw, hemp shiv and rice husk.

29

30 Table 1 - Bulk density values, water adsorption and thermal conductivity for barley straw, hemp shiv and rice husk fibres.

	Barley straw (S)	Hemp shiv (H)	Rice husk (RH)
Bulk density (kg/m ³)	574	153	85,09
Water absorption (%)	414	380	300
Thermal conductivity (W/(mK))	0,044	0,051	0,056

1

2 Barley straw and hemp shiv fibres characterisation was presented elsewhere by Laborel-Préneron et al. (2017a). In order to
 3 calculate the bulk density of a rice husk sample, the fibres were sieved and dried at 60°C until the weight variation was less
 4 than 0.1% within two weighing's 24h apart. Then a cup with 0.749 dm³ was filed with rice husk and weight three times. The
 5 bulk density is determined by the quotient between the measured mass (g) and the recipient volume (m³). The bulk density of
 6 the rice husk particles was given by the average value between the three measurements.

7 The rice husk thermal conductivity was measured with an ISOMET 2104 Heat Transfer Analyzer equipment. A PVC mould
 8 with 40 mm high and diameter 100 mm was field with rice husk and the thermal conductivity coefficient determined with
 9 resource to a probe with ranging values between 0.04-0.3 W/m.K (Figure 2). The rice husk sample was previously sieved and
 10 dried in the same conditions earlier described.

11 The water absorption was measured for three rice husk samples with 25 g, previously sieved and dried in the conditions
 12 described for bulk density and thermal conductivity. Then the samples were placed in tule bags and immersed in water for 15
 13 minutes, 4 and 48 hours. After the immersing time the samples were drained on the bags and their weight measured. Finally,
 14 the water absorption ratio in function of time is determined based on equation 1.

$$15 \quad w(t) = \frac{m(t) - m_0}{m_0} \times 100 \quad (1)$$

16



17

18 **Figure 2 – Rice husk thermal conductivity test.**

19 The main chemical compounds are presented in (Laborel-Préneron et al. 2017c and Rosario Madrid 2009).
 20 They were measured and by the Eurofins company using the Van Soest method, according to standard NF V18-
 21 122 (AFNOR 2013). This test provides 3 results: NDF (Neutral Detergent Fibre), corresponding to the total fibre;
 22 ADF (Acid Detergent Fibre), which contains mainly cellulose and lignin; and ADL (Acid Detergent Lignin),
 23 corresponding to the lignin. Measurement uncertainties were 10% for NDF and ADF and 15% for ADL. Cellulose
 24 and hemicellulose were thus calculated by the subtractions ADF-ADL and NDF-ADF, respectively. The chemical
 25 characterisation of the tested fibres are presented below in Table 2.

26

27 **Table 2 - Chemical characterisation of the tested fibres: barley straw, hemp shiv and rice husk fibres.**

Aggregate	Reference	Lignin (%)	Cellulose (%)	Hemicellulose (%)	Extractives (%)	Ash (%)
Barley straw	(Laborel-Préneron et al. 2017c)	5,5	37,7	26,7	14,4	12,3
Hemp shiv	(Laborel-Préneron et al. 2017c)	17,2	50,3	17,9	5,9	2,1
Rice husk	(Rosario Madrid 2009)	33	30	20	3	14

1

2

3

4 2.1.2. Earth

5 The earth used for block production is composed by quarry fines from washing aggregate sludge obtained from the washing
6 of limestone aggregates produced for the concrete industry. The Atterberg limits of this material were previously determined
7 by Laborel-Préneron (2017) and the mineralogical composition is referred by Laborel-Préneron et al. (2018) (table 3). The dry
8 density of the earth was measured by the same method adopted for rice husk fibres and is also presented in table 3.

9 Table 3 - Atterberg limits and mineralogical composition of earth (Laborel-Préneron 2017), (Laborel-Préneron et al. 2018).

Atterberg limits	
W _L (%)	30
W _P (%)	21
PI (%)	9
Mineralogic composition	
Calcite (%)	63
Dolomite (%)	3
Kaolinite (%)	11
Quartz (%)	10
Illite (%)	9
Goethite (%)	3
Dry density	
ρ (g/m ³)	0,756

10

11

12 The particle size distribution and the granulometric curve of the earth was calculated by using a sample of 1 kg which was
13 dried until the mass was constant with less than 0.1% weight variation within two weighings 24 hours apart. The sample was
14 shaken through a defined set of sieves with different openings for 2 minutes; after that, the retained percentage of earth in
15 each sieve was determined resulting on the particle size distribution curve (figure 3).

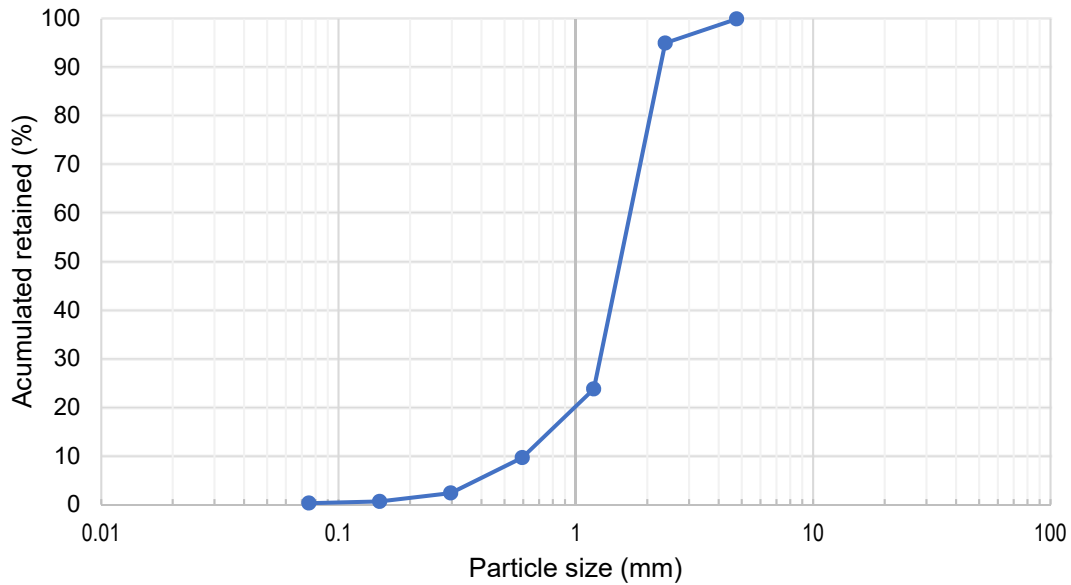


Figure 3 - FWAS granulometric curve.

2.1.3. Gypsum and air lime used in the blocks

The hemihydrated gypsum used to stabilise some of the blocks was from Sival and the air lime was a CL-90 S from Lusalcal, Lhoist Group (Table 4).

Table 43 - Gypsum properties.

Gypsum properties	
Water/gypsum ration (kg/l)	1,25
Hardness time (min)	13 ± 4
Linear expansion (1h) (%)	max 0,20
Tensile flexural strength (kg/cm ²)	40

2.2 Tests procedures

2.2.1 Casting and curing

Three specimens for the different tests were prepared by two different casting methods for the manufacturing of blocks with a fibre content of 3% (in weight): method one for 20x20x5 cm³ unstabilised statically compressed earth blocks with barley straw, hemp shiv and rice husk, and method 2 for 20x20x4 cm³ gypsum and air lime stabilised hand moulded earth blocks with the same rice husk as before.

The water contents of the mixtures for 5 cm thickness compressed blocks were determined by the Proctor test, and then rounded up because this is a minimum value for manufacturing compressed earth bricks (Laborel-Préneron et al. 2017b); Laborel-Préneron et al. 2018). For this 1st method, as it was expected, the water content of the dry mass needed to make the mixtures was higher for straw than for hemp and rice husk because straw particles have a higher water absorption coefficient than the other two aggregates (Table 1).

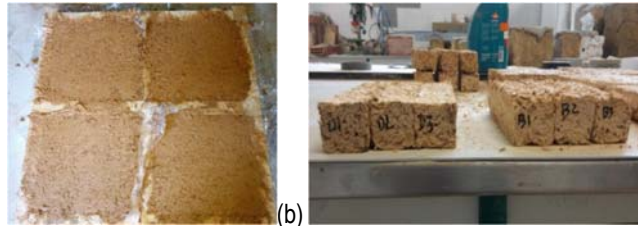
In the second casting process for the 4 cm thickness moulded blocks production, the dry ingredients – earth, gypsum and lime – were mixed with a shovel. Water was then added while mixing with a mechanical mixer until the mixture was homogenised letting the mixture to flow into the mould. Since the composition includes gypsum, which has a very quick hardening process, the protocol was based on Lima et al. (2016) and the earth-binder-water mixture was mixed during 90 seconds. The rice husk was then added to the mixture and mixed mechanically with the same device until a homogeneous consistency was obtained (around 1 minute). The specimens were casted on 20x20x4 cm³ wooden moulds (Figure 5a). To simplify and to avoid fractures

1 on the demoulding process, a transparent plastic paper was wrapped around the wooden moulds. Figure 4 presents a scheme
2 of the casting method. The specimens were casted on 20x20x4 cm wooden moulds.



3

(a)



4

(b)

(c)

5 Figure 4 - Casting method adopted for method 2 (representative) (a); block (b) and prismatic (c) rice husk specimens.

6 After casting the 4 cm specimens were left to dry at laboratory conditions with 23°C temperature and 50% RH. The blocks
7 were demoulded after 2 weeks curing and let to dry for two more weeks.

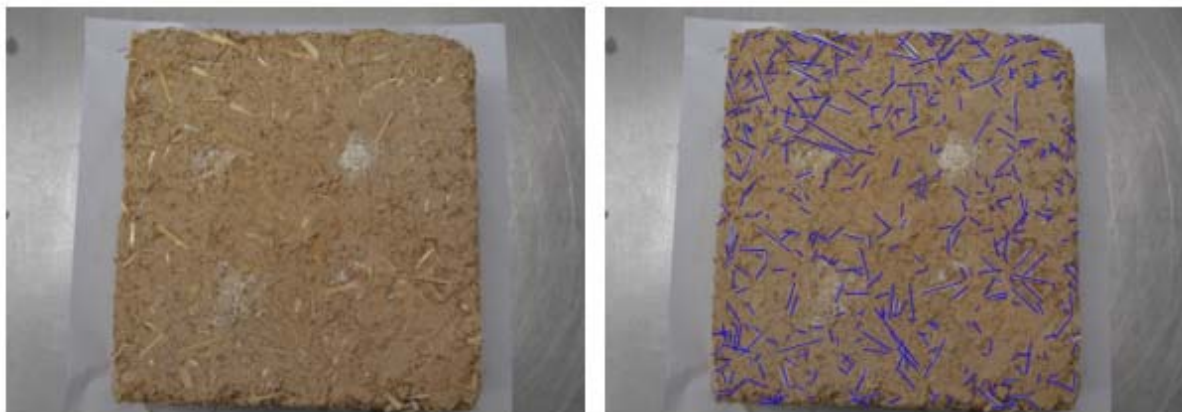
8

9 2.2.2 2D image analysis.

10 According to the literature review, ImageJ is commonly used on image analysis; so for the present study it was used this
11 software tool. Because of the colours similarity between the fibres and the earth matrix, and the difficulty on knowing the shape
12 of the fibres, a segmentation process was not a possibility, making it impossible to perform an automatically analysis of the
13 block surface.

14 First it was taken a high-quality picture with a 15 megapixels' camera; then the contrast was slightly adjusted for better
15 perception of the fibres outline from the earthen matrix. Resourcing to ImageJ a scale was set based on the horizontal
16 dimension of the blocks; finally the length and the angle of orientation with the horizontal plane were measured for each fibre
17 (Figure 5).

18 The objective was to determine the influence of fibre length and orientation on the thermal conductivity and ultra sound
19 propagation properties of the earth blocks. It is important to retain that this method is made manually for about 400 fibres in
20 each surface; whereby there is an error associated to these measurements.



21

22

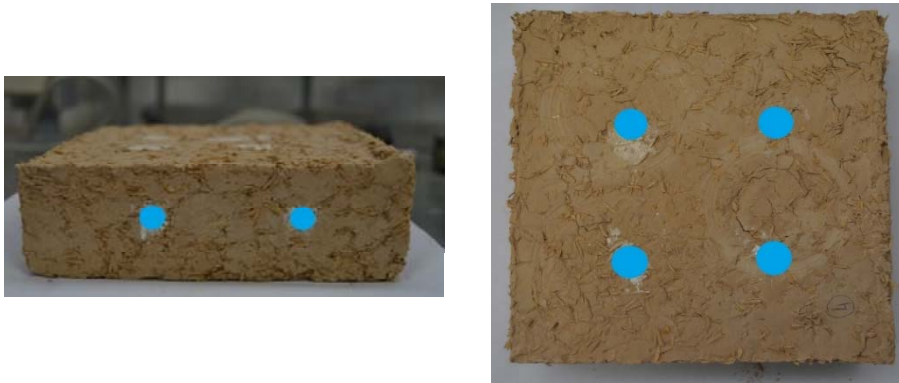
Figure 5 – Example of a barley straw block before and after Image J analysis.

1 2.2.3 Thermal conductivity and bulk density

2 To determine the thermal conductivity of the earth blocks the same equipment described previously for the rice husk thermal
3 conductivity was used. The specimens were stored in laboratory-controlled conditions at 23°C and 50% relative humidity (RH)
4 to reach equilibrium with the environment. A probe with 0.3-0.6 W/(m.K) range values was used for the 5 cm thick blocks, and
5 the thermal conductivity was measured firstly in 3 points. After the first measurements, it was showed that the measurement
6 on three points was irrelevant, once the difference was reduced; so the blocks were measured only on a central point. Once
7 the results showed differences less than 0.1% from each other the measurements were only taken on the centre of the blocks.
8 For the 4 cm thick blocks, five initial points were measured using a 0.04-0.3 W/(m.K) probe: four points on the vertices and
9 one at the centre of the panels. Three measurements were performed on each point.

1 2.2.4 Ultra sound propagation velocity

2 The ultra sound propagation velocity assesses the internal structure of the earth blocks and can induce its durability. The test
3 was conducted based on the EN 12504-4 with a Proceq Pundit Lab equipment. The time that the impulse takes between two
4 transducers, placed on opposite faces for direct measurements and on the same face for indirect measurements, was
5 measured. Measurements were made in four points in the top face and two on each lateral side (figure 6).



6 Figure 6 - Measurement points for ultra sound propagation speed.

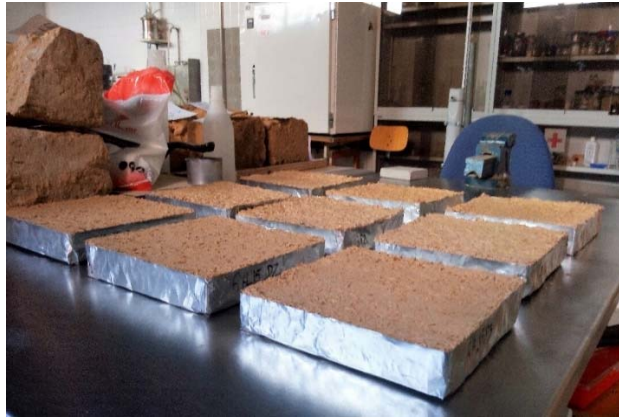
6

7 It was not possible to perform the ultra sound test to all blocks once some specimens were damaged, presenting some internal
8 fractures. 3 specimens were tested for each formulation.

9 2.2.5 Moisture buffering test

10 The Moisture Buffer Value (MBV) is a characteristic of the material based on the adsorption and desorption of moisture. It
11 translates the ability of the material to regulate indoor air humidity (Ramos 2007). The MBV concept was developed by a
12 Norden group of investigators within NORDTEST (Rode et al. 2005) which also defines the MBV experimental protocol for its
13 determination.

14 For each formulation, 3 specimens were tested.. They were wrapped in aluminium tape, leaving only one surface free and let
15 to stabilise for 5 days (Figure 7). Then the specimens were exposed to RH cycles of 60% for 16h to 90% for 8h at 16°C
16 temperature. This temperature is low but was measured in unheated dwellings in Portugal.



1

2

Figure 7 - Blocks pre-conditioning for the moisture buffering test.

3. Results and Discussion

3.1. 2D Image Analysis – ImageJ

The fibre length and orientation of 20x20x4 and 5 cm blocks were measured using a 2D Image analysis software for all the compositions (barley straw, hemp shiv and rice husk with two different thicknesses). It enabled to calculate an average and frequency distribution of the obtained results. The following figures present the results for barley straw blocks, hemp shiv blocks and rice husk blocks.

The fibre length and orientation angle orientation distribution (frequency in bars, cumulative distribution in lines) of barley straw blocks are presented in Figs. 8a and 8b.

10

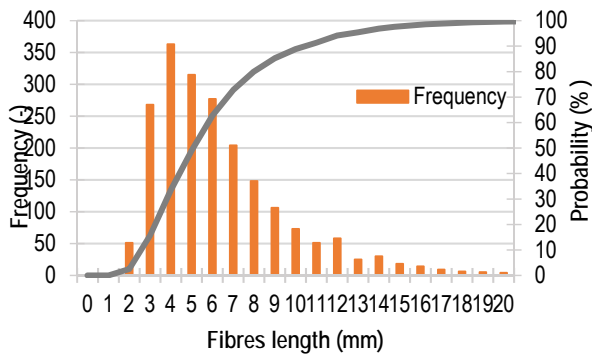


Figure 8a - Fibre length distribution for barley straw 5 cm thickness blocks.

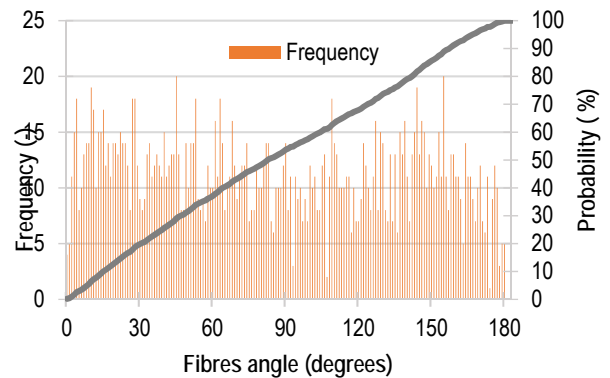


Figure 8b - Fibre angle distribution for barley straw 5 cm thickness blocks.

The fibre length and orientation angle distribution of hemp shiv blocks are presented in Figs. 9a and 9b.

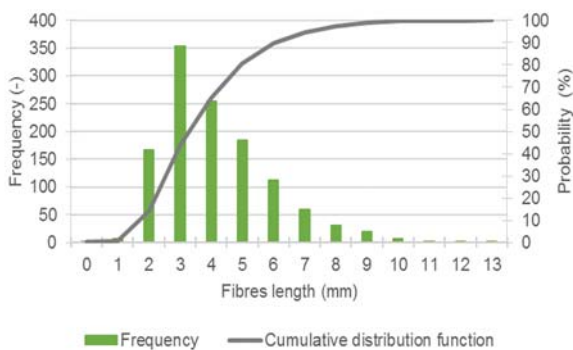


Figure 9a - Fibre length distribution for hemp shiv 5 cm thickness blocks.

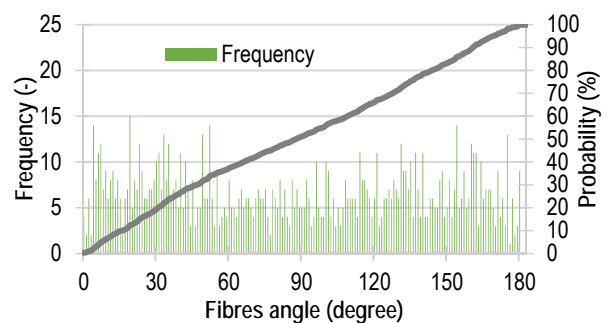


Figure 9b - Fibre angle distribution for hemp shiv 5 cm thickness blocks.

1 The fibre length and orientation angle distribution of rice husk blocks are presented in Figs. 10a and 10b.

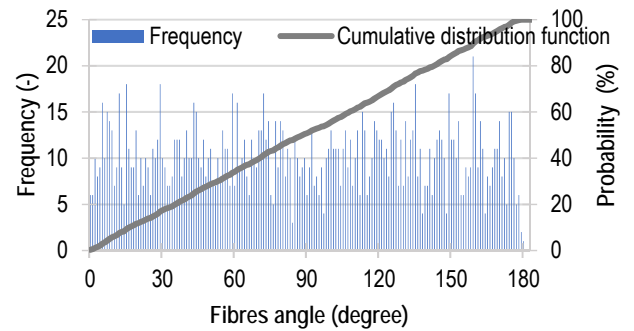
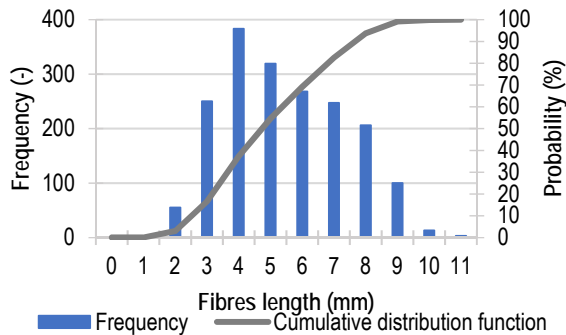


Figure 10a - Fibre length distribution for rice husk blocks with 5 cm thickness.

Figure 10b - Fibre angle distribution for rice husk blocks with 5 cm thickness.

1

2 Figs. 11a and 11b present the fibre length and the orientation angle distribution for rice husk blocks with 4 cm thickness, respectively.

3

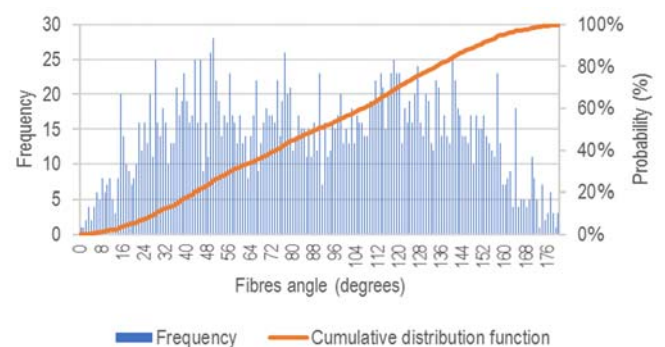
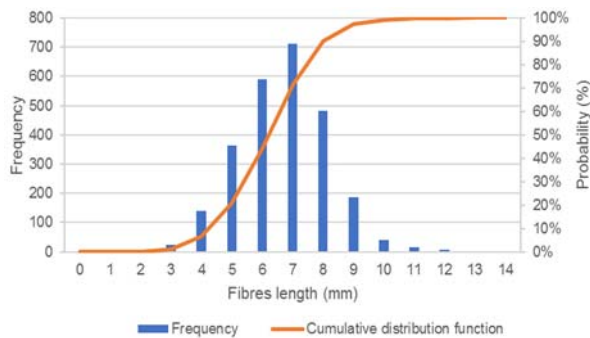


Figure 11a - Fibre length distribution for rice husk blocks with 4 cm thickness.

Figure 11b - Fibre angle distribution for rice husk blocks with 4 cm thickness.

1 The previous figures show that the probability of achieving a specific fibre length tends to a lognormal distribution. Beside this,
 2 the probability of achieving a fibre angle orientation between 0° or 90° degrees is the same, meaning that a uniform distribution
 3 is detected for the fibre angle distribution. The average length of barley straw fibres is 5 mm and for hemp shiv fibres is around
 4 3.5 mm.

5 Regarding the fibre angle in the rice husk 4 cm blocks it is shown that the casting method can have a strong influence on the
 6 fibres orientation. Figure 11b demonstrates that the fibre orientation distribution is not uniform and so the probability of
 7 achieving a fibre angle orientation of 0° or 90° is not the same.

8 The comparison of Figure 10a and Figure 11a shows that the different casting of the products have stronger influence on the
 9 fibre length, although the same type of fibre was used in both compositions. The different casting methods used for the rice
 10 husk blocks with a thickness of 4 cm and 5 cm can break the fibres (5 mm length in the compressed blocks, with higher
 11 thickness, and 6 mm in the moulded ones, with 4 cm), leading to different physical characteristics. It is also possible to see
 12 that an optimised casting method, as the one used on the rice husk blocks with 4 cm, could lead to a more homogeneous fibre
 13 distribution and microstructure, although to a lower compaction.

14 3.2. Thermal conductivity

15 The thermal conductivity of barley straw and hemp shiv blocks is in the same ranging values, about 0.26 ± 0.01 W/(m.K); on
 16 the other hand the rice husk blocks showed higher thermal conductivity- 0.53 W/m.K. It is possible to see a relation between

1 this parameter and the geometrical properties of the natural fibres. According to Laborel-Préneron (2017) barley straw fibres
 2 have the higher diameter and length, followed by hemp shiv and rice husk. Therefore, it is shown that that the largest fibres
 3 lead to lower and better thermal conductivity values.

4 The geometrical properties of natural fibres seem to be directly connected to the bulk density of the earth blocks: the bigger
 5 the fibres, the lower the bulk density, leading to lower thermal conductivity of the composite (Table 5).

6

7

Table 5 - Blocks thermal conductivity as a function of bulk density.

Specimen	λ_{average} (W/m.K)	Standard deviation (W/m.K)	Bulk density(kg/m ³)	Fibres length average (mm)
Barley straw 20x20x5 cm ³ (S)	0.261	0.050	1490	5
Hemp shiv 20x20x5 cm ³ (H)	0.269	0.057	1518	3.5
Rice husk 20x20x5 cm ³ (RH)	0.530	0.051	1808	5
Rice husk 20x20x4 cm ³	0.102	0.010	651	6

8

9 Through the analysis of Table 5 and making a comparison with the distribution curves obtained for the fibres length and
 10 orientation (Figs. 12 to 19) combined with fibres characterisation (table 1), it is possible to see that the fibre length could have
 11 an influence on the thermal conductivity of the composites. Rice husk thermal conductivity is higher than for barley straw and
 12 hemp shiv, but an optimised casting method can lead to a substantial thermal conductivity reduction of the block composite
 13 (0,102 W/(mK)). Larger the area occupied with natural fibres, the higher the effect that it will have on the thermal behaviour of
 14 the composite. However, the orientation angle of the fibres seems to be an irrelevant factor for this property. An optimised
 15 casting method, as the one used on the rice husk blocks with 4 cm – moulding instead of compaction - could lead to a more
 16 homogeneous fibre distribution, which contributes to a lower and optimised thermal conductivity of the blocks. Nevertheless
 17 that can have drawbacks on mechanical characteristics, that will be addressed elsewhere.

18 3.3. Moisture Buffer Test

19 In order to compare the impact of different casting methods on the moisture buffering of rice husk blocks, 20x20x5 cm³ rice
 20 husk blocks were compared with the ones with 20x20x4 cm³. MBV curves were obtained at the stabilised stage. Figure 12
 21 shows that the MBV of 5 cm thickness blocks is higher than the ones with 4 cm, but both present an excellent hygroscopic
 22 behaviour. Table 6 present the moisture buffering value for the rice husk blocks.

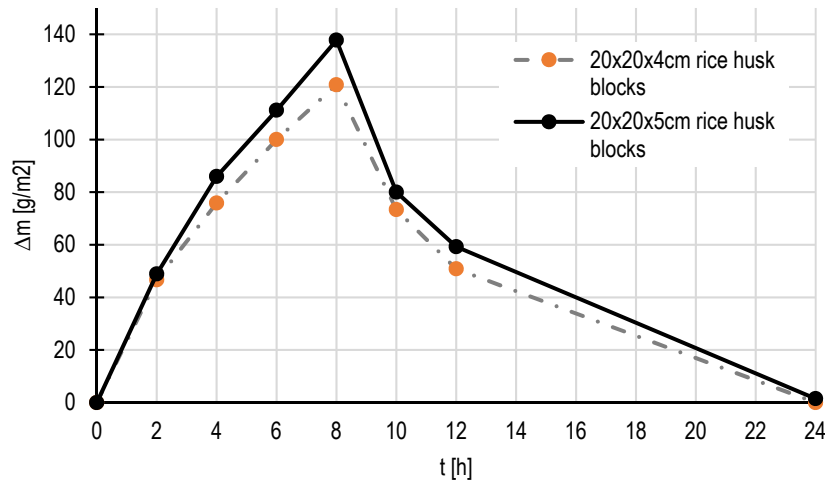


Figure 12 - Stabilised adsorption and desorption moisture buffering curves for rice husk blocks with the two casting methods.

Table 6 - Moisture buffering value for the rice husk blocks – stabilised cycle.

	4 cm rice husk blocks	5 cm rice husk blocks
MBV	4.11	4.54

The previous results show that the different casting method seems to slightly change MBV. Beside this, the different thickness could also contribute to that change. This is in agreement with McGregor et al. (McGregor et al. 2014) where it was shown that there was no significant difference for the MBV between materials of different thicknesses (30, 50 and 70mm). The adsorption curve of the 20x20x4 cm³ rice husk blocks show that the specimens present their maximum adsorption value lower than the 20x20x5 cm³ blocks.

3.4. Ultra sound propagation velocity

Figures 13 and 14 show the ultra sound velocity results for the three specimens of barley straw, hemp shiv and rice husk (with two different casting methods). Two different measurements were made, the direct measurements where the transducers are placed in opposite surfaces and the indirect measurements with both transducers on the same surface. The average values and the frequency distribution curve were calculated for both direct and indirect methods.

The following figures present the results for barley straw blocks and Figs. 14a and 14b for hemp shiv blocks.

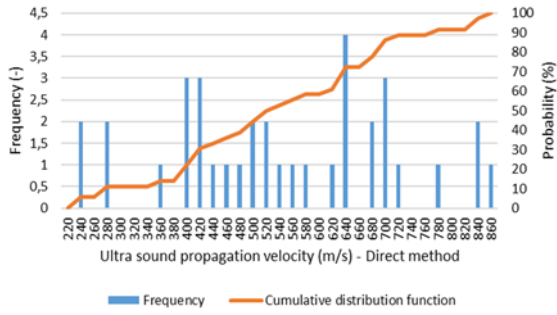


Figure 13a - Ultra sound propagation velocity distribution for 5 cm barley straw blocks - Direct method.

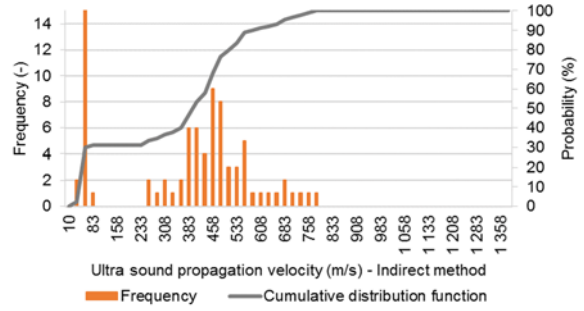


Figure 13b - Ultra sound propagation velocity distribution for 5 cm barley straw blocks - Indirect method.

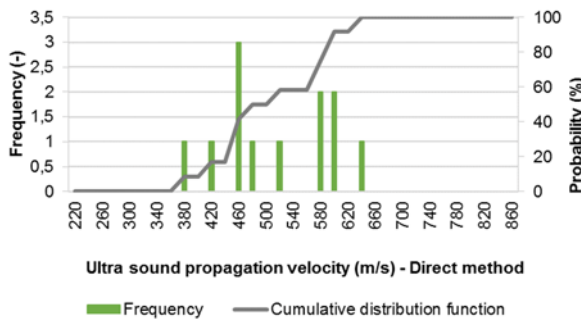


Figure 14a - Ultra sound propagation velocity distribution for 5 cm hemp shiv blocks - Direct method.

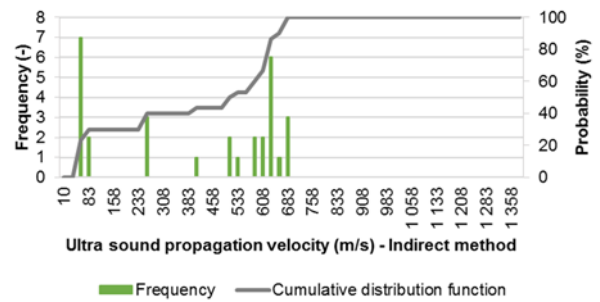


Figure 14b - Ultra sound propagation velocity distribution for 5 cm hemp shiv blocks - Indirect method.

1 The hemp shiv blocks present the higher propagation velocity in comparison with the barley straw blocks, which is correlated
 2 with a higher density of the composite. The lack of results in the previous figures 14a and 14b are due to some fractures
 3 observed in the blocks that did not enable to get as much results as in the barley straw blocks. It seems that the direct method
 4 gives more information than the indirect method for ultra sound propagation velocity as the range of velocities is higher.
 5 However, both enable to define a probabilistic distribution function.

6 The rice husk blocks frequency and distribution curves, for ultra sound results are presented in Figures 15a and 15b.

7

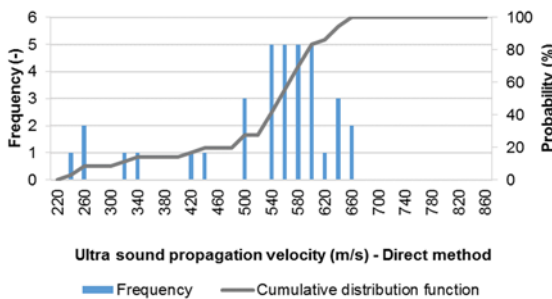


Figure 15a - Ultra sound propagation velocity distribution for 5 cm rice husk blocks - Direct method.

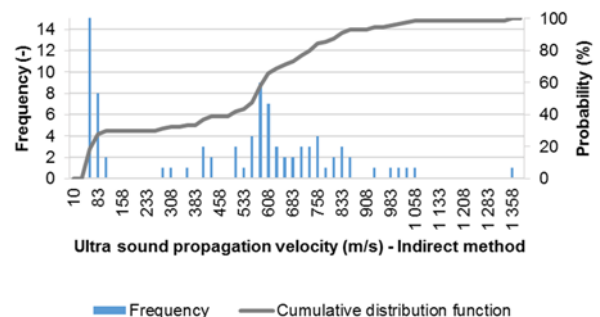


Figure 15b - Ultra sound propagation velocity distribution for 5 cm rice husk blocks - Indirect method.

1 Rice husk blocks with 5 cm present a higher range of velocities in comparison with barley straw and hemp shiv blocks.
 2 However, the average value of ultra sound velocity is higher in rice husk blocks, which is associated with a higher density and
 3 mechanical strength.

4 For the 4 cm rice husk blocks the frequency and distribution curves of the ultra sound results are presented in Figure 16a and
 5 16b.

6

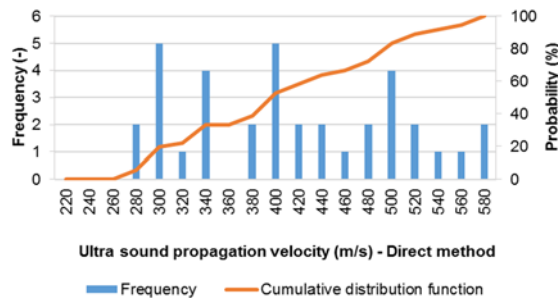


Figure 16a - Ultra sound propagation velocity distribution for 4 cm rice husk blocks - Direct method.

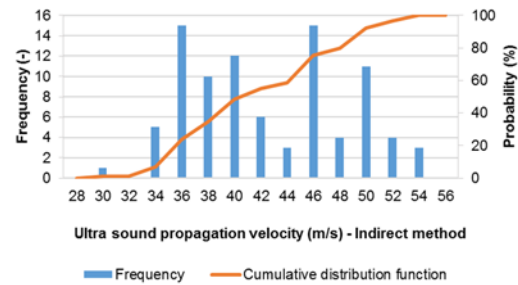


Figure 16b - Ultra sound propagation velocity distribution for 4 cm rice husk blocks - Indirect method.

1 The previous results show that ultra sound velocity is higher for the 5 cm rice husk specimens, increasing with the increase of
 2 bulk density. The barley straw and hemp shiv blocks were more porous, explaining the lower values. The same explanation is
 3 found for 4 cm rice husk blocks, as these ones have lower ultra sound velocity and higher porosity, which is in agreement with
 4 the better thermal behaviour. In comparison with 5 cm rice husk blocks, the results obtained for the 4 cm rice husk blocks
 5 suggest that the casting method can have a strong influence on the properties of the composites.

6 The distribution curve obtained for both direct and indirect method is not similar, showing that the internal structure of the
 7 panels is not uniform in different directions, which may be related to the casting method used. The shape of the ultra sound
 8 velocity distribution from direct and indirect method enhance the anisotropy of the bio-based materials with different casting
 9 methods.

10 Like thermal conductivity, the ultra sound results are directly connected to the bulk density of the blocks; so it is also possible
 11 to establish a relation between these results and the geometry of the fibres. Widest and longest fibres will lead to a more porous
 12 block, leading to a lower propagation velocity like barley straw, inducing that these will have lower durability. On the contrary,
 13 the rice husk blocks being the less porous and more homogenous specimens should have better durability properties.

14 These results are on the same page as Laborel-Préneron (2017) results, where rice husk also had the highest propagation
 15 velocity, followed by the hemp shiv and finally the barley straw. The results indicate that production variables have a significant
 16 directionally dependent impact on the physical properties of cast bio-based materials. Thermal conductivity and ultra sound
 17 velocity are affected by fibres distribution inside bio-based materials. This means that the Image analysis can be used for
 18 quality control towards the optimisation of the bio-composites. However, it is clear that there is a strong opportunity to improve
 19 the technique by using a 3D analysis in the materials.

20 5. Conclusion

21 Specimens for the different tests were prepared by two casting methods for the manufacturing of blocks with a fibre content of
 22 3% (in weight): compaction method for 20x20x5 cm³ blocks (barley straw, hemp shiv and rice husk) and manual moulding
 23 method for 20x20x4 cm³ rice husk blocks. 2D image analysis was used in the hardened samples to determine the influence
 24 of fibre length and orientation on the thermal conductivity and ultra sound propagation properties of the earth blocks. A brief
 25 analysis to moisture buffering behaviour of rice husk-based samples is also presented.

26 The 4 cm rice husk blocks demonstrate that the casting method can have a strong influence on the fibres orientation. The fibre
 27 orientation distribution is not always uniform in the bio-based composite tested and the probability of achieving a fibre angle
 28 of 0° or 90° is not the same.

1 For barley straw and hemp shiv blocks, the average length of barley straw fibres is 5 mm and for hemp shiv fibres is around
2 3.5 mm and uniform distribution was detected for fibres orientation. The different casting methods used for the rice husk blocks
3 with a thickness of 4 cm and 5 cm have shown that the compaction method can break the fibres (fibres average length of 5
4 mm in the 5 cm compacted blocks and 6 mm in the moulded ones with 4 cm), leading to different physical characteristics.

5 Rice husk fibres thermal conductivity is higher than for barley straw and hemp shiv, but an optimised casting method can lead
6 to a substantial thermal conductivity reduction of the block composite (0,102 W/(mK) for 4 cm rice husk blocks). Larger the
7 area occupied with natural fibres, the higher the effect that it will have on the thermal behaviour of the composite. The results
8 also demonstrate that MBV is slightly affected by fibres distribution inside bio-based materials. An optimised casting method,
9 as the one used on the 4 cm moulded rice husk blocks, could lead to a more homogeneous fibre distribution, which contributes
10 to a lower and optimised thermal conductivity of the blocks.

11 Based on the image analysis method it was seen that the length and orientation of the natural fibres could have influence on
12 the ultra sound propagation velocity results and, in this way, on the durability and thermal performance of earth composites.
13 Longer fibres lead to a decrease in bulk density, thermal conductivity and ultra sound propagation velocity when compared
14 with shorter fibres. The shape of the ultra sound velocity distribution from direct and indirect method can enhance the
15 anisotropy of the bio-based materials with different casting methods. Although, there is space for improvement of the technique
16 as the main weakness of the research is that only a bidimensional analysis is provided. A 3D analysis will easily detect the
17 anisotropic behaviour of the analysed properties.

18 An optimised production process could be the key to the production of high performance bio-based materials.

19

20 Acknowledgement

21 The authors gracefully acknowledge the help given by the Eng. Vitor Silva throughout the experimental campaign. This work
22 is developed within RILEM Technical Committees 274 TCE and 275 HDB.

23

24 References

25 (Asdrubali et al. 2016) Asdrubali, F., Bianchi, F., Cotana, F., D'Alessandro, F., Pertosa, M., Pisello, A. L., & Schiavoni, S.
26 (2016). Experimental thermo-acoustic characterisation of innovative common reed bio-based panels for building envelope.
27 *Building and Environment*, 102, 217–229. <https://doi.org/10.1016/j.buildenv.2016.03.022>

28 (Minke 2006) Minke, G. (2006). *Building with Earth. Design and technology of a sustainable Architecture*, Birkhauser. ISBN:
29 3-7643-7477-2

30 (McGregor et al. 2014) McGregor, F., Heath, A., Fodde, E., & Shea, A. (2014). Conditions affecting the moisture buffering
31 measurement performed on compressed earth blocks. *Building and Environment*, 75, 11–18.
32 <https://doi.org/10.1016/j.buildenv.2014.01.009>

33 (Binici et al. 2005) Binici, H., Aksogan, O., & Shah, T. (2005). Investigation of fibre reinforced mud brick as a building material.
34 *Construction and Building Materials*, 19(4), 313–318. <https://doi.org/10.1016/j.conbuildmat.2004.07.013>

35 (Aymerich et al. 2012) Aymerich, F., Fenu, L., & Meloni, P. (2012). Effect of reinforcing wool fibres on fracture and energy
36 absorption properties of an earthen material. *Construction and Building Materials*, 27(1), 66–72.
37 <https://doi.org/10.1016/j.conbuildmat.2011.08.008>

38 (Laborel-Préneron et al. 2016) Laborel-Préneron, A., Aubert, J. E., Magniont, C., Tribout, C., & Bertron, A. (2016). Plant
39 aggregates and fibers in earth construction materials: A review. *Construction and Building Materials*, 111, 719–734.
40 <https://doi.org/10.1016/j.conbuildmat.2016.02.119>(Brouard et al 2018) Brouard Y., Balayachi N., Hoxha D., Ranganathan N.,
41 Méo S. (2018). Mechanical and hygrothermal behavior of clay-sunflower (*Helianthus annuus*) and rape straw (*Brassica napus*)
42 plaster bio-composite for building insulation. *Construction and Building Materials* 161, 196-207.
43 <https://doi.org/10.1016/j.conbuildmat.2017.11.140>

44 (Gullu & Khudir 2014) Güllü, H., & Khudir, A. (2014). Effect of freeze-thaw cycles on unconfined compressive strength of fine-
45 grained soil treated with jute fiber, steel fiber and lime. *Cold Regions Science and Technology*, 106–107, 55–65.
46 <https://doi.org/10.1016/j.coldregions.2014.06.008>

47 (Rim et al. 1999) Al Rim, K., Ledhem, A., Douzane, O., Dheilly, R. M., & Queneudec, M. (1999). Influence of the proportion of
48 wood on the thermal and mechanical performances of clay-cement-wood composites. *Cement and Concrete Composites*,
49 21(4), 269–276. [https://doi.org/10.1016/S0958-9465\(99\)00008-6](https://doi.org/10.1016/S0958-9465(99)00008-6)

50 (Obonyo et al. 2010) Obonyo, E., Exelbirt, J., & Baskaran, M. (2010). Durability of compressed earth bricks: Assessing erosion

1 resistance using the modified spray testing. *Sustainability*, 2(12), 3639–3649. <https://doi.org/10.3390/su2123639>

2 (Binici et al. 2007) Binici, H., Aksogan, O., Bodur, M. N., Akca, E., & Kapur, S. (2007). Thermal isolation and mechanical
3 properties of fibre reinforced mud bricks as wall materials. *Construction and Building Materials*, 21(4), 901–906.
4 <https://doi.org/10.1016/j.conbuildmat.2005.11.004>

5 (Achenza & Fenu 2007) Achenza, M., & Fenu, L. (2007). On Earth Stabilization with Natural Polymers for Earth Masonry
6 Construction. *Materials and Structures*, 39, 21–27. <https://doi.org/10.1617/s11527-005-9000-0>

7 (Antunes et al. 2017) Antunes, A., Faria, P., Brás, A., Silva, V. (2017). Performance of bio-based insulation panels. Final COST
8 Action FP 1303 International Conference "Building with bio-based materials: Best practice and performance specification".
9 Zivkoviv, V., Jones, D. (Eds.). Zagreb, Croatia, 6-7 Septembre 2017, p. 58-59. ISBN:978-953-292-051-2 (Extended abstracts)

10 (Lima and Faria, 2016) Lima, J., Faria, P. (2016), Eco-efficient earthen plasters. The influence of the addition of natural fibers.
11 *Natural Fibres: Advances in Science and Technology Towards Industrial Applications. From Science to Markets*, Fangueiro,
12 Raul, Rana, Sohel (Eds.). Springer, RILEM Book Series vol. 12, 315-327, Doi:10.1007/978-94-017-7515-1_24

13 (Faria et al. 2016) Faria, P., dos Santos, T., & Aubert, J.-E. (2016). Experimental Characterization of an Earth Eco-Efficient
14 Plastering Mortar. *Journal of Materials in Civil Engineering*, 28(english). [https://doi.org/10.1061/\(ASCE\)MT.1943-5533.0001363](https://doi.org/10.1061/(ASCE)MT.1943-5533.0001363).

15

16 (Williams et al 2016) Williams, J., Lawrence, M., Walker, P. (2016). A method for the assessment of the internal structure of
17 bio-aggregate concretes, *Construction and Building Materials*, 116, 45-51, <https://doi.org/10.1016/j.conbuildmat.2016.04.088>

18 (Nguyen et al 2010) Nguyen, T.T., Picandet, V., Carre, P., Lecompte, T., Amziane, S., Baley, C. (2010). Effect of compaction
19 on mechanical and thermal properties of hemp concrete, *Eur. J. Environ. Civ. Eng.* 14 (5), 545–560.
20 <https://doi.org/10.1080/19648189.2010.9693246>

21 (Dinh et al. 2015) Dinh, T.; Magniont, C., Coutand, M., Escadeillas, G. (2015). Hemp concrete using innovative pozzolanic
22 binder. 1st International Conference on Bio-based Building Materials, Clermont-Ferrand, France.

23 (Pierre et al. 2014) Pierre, T., Colinart, T., Glouannec, P. (2014). Measurement of thermal properties of biosourced building
24 materials, *Int. J. Thermophys.* 35 (9–10), 1832–1852. <https://doi.org/10.1007/s10765-013-1477-0>

25 (Millogo et al. 2014) Millogo, Y., Morel, J. C., Aubert, J. E., & Ghavami, K. (2014). Experimental analysis of Pressed Adobe
26 Blocks reinforced with Hibiscus cannabinus fibers. *Construction and Building Materials*, 52, 71–78.
27 <https://doi.org/10.1016/j.conbuildmat.2013.10.094>

28 (Bouguerra et al. 1998) Bouguerra, A., Ledhem, A., Barquim, F., Dheilly, R.M., Quéneudec, M. (1998). Effect of
29 Microstructure on the Mechanical and Thermal Properties of Lightweight concrete prepared from clay, cement, and wood
30 aggregates. *Cement and Concrete Research*, 28(8), 1179–1190. [https://doi.org/10.1016/S0008-8846\(98\)00075-1](https://doi.org/10.1016/S0008-8846(98)00075-1)

31 (Khedari et al. 2005) Khedari, J., Watsanasathaporn, P., & Hirunlabh, J. (2005). Development of fibre-based soil-cement block
32 with low thermal conductivity. *Cement and Concrete Composites*, 27(1), 111–116.
33 <https://doi.org/10.1016/j.cemconcomp.2004.02.042>

34 (Ledhem et al. 2000) Ledhem, A., Dheilly, R. M., Benmalek, M. L., & Quéneudec, M. (2000). Properties of wood-based
35 composites formulated with aggregate industry waste. *Construction and Building Materials*, 14(6–7), 341–350.
36 [https://doi.org/10.1016/S0950-0618\(00\)00037-4](https://doi.org/10.1016/S0950-0618(00)00037-4)

37 (Bessa et al. 2012) Bessa, I. S., Castelo Branco, V. T. F., & Soares, J. B. (2012). Evaluation of different digital image processing
38 software for aggregates and hot mix asphalt characterisations. *Construction and Building Materials*, 37, 370–378.
39 <https://doi.org/10.1016/j.conbuildmat.2012.07.051>

40 (Yoo et al. 2016) Yoo, D. Y., Banthia, N., Kang, S. T., & Yoon, Y. S. (2016). Effect of fiber orientation on the rate-dependent
41 flexural behavior of ultra-high-performance fiber-reinforced concrete. *Composite Structures*, 157, 62–70.
42 <https://doi.org/10.1016/j.compstruct.2016.08.023>

43 (Sebaibi et al. 2014) Sebaibi, N., Benzerzour, M., & Abriak, N. E. (2014). Influence of the distribution and orientation of fibres
44 in a reinforced concrete with waste fibres and powders. *Construction and Building Materials*, 65, 254–263.
45 <https://doi.org/10.1016/j.conbuildmat.2014.04.134>

46 (Laborel-Préneron et al. 2017a) Laborel-Préneron, A., Magniont, C., & Aubert, J. E. (2017a). Characterisation of barley straw,
47 hemp shiv and corn cob as resources for bioaggregate based building materials. *Waste and Biomass Valorization*, 0(0), 1–18.
48 <https://doi.org/10.1007/s12649-017-9895-z>

49 (Amziane et al. 2017) Amziane, S., Collet, F., Lawrence, M., Magniont, C., Picandet, V., & Sonebi, M. (2017). Recommendation
50 of the RILEM TC 236-BBM: characterisation testing of hemp shiv to determine the initial water content, water absorption, dry
51 density, particle size distribution and thermal conductivity. *Materials and Structures/Materiaux et Constructions*, 50(3).

1 <https://doi.org/10.1617/s11527-017-1029-3>

2 (Laborel-Préneron 2017) Laborel-Préneron, A. (2017). Formulation and characterisation of unfired clay bricks with plant
3 aggregates. PhD thesis, Université Paul Sabatier , Toulouse.

4 (Laborel-Préneron et al. 2018) Laborel-Préneron, A., Magniont, C., Aubert, J.-E. (2018). Hygrothermal properties of unfired
5 earth bricks: effect of barley straw, hemp shiv and corn cob addition. Energy and Buildings (in press).
6 <https://doi.org/10.1016/j.enbuild.2018.08.021>

7 (Laborel-Préneron et al. 2017b) Laborel-Préneron, A., Aubert, J.-E., Magniont, C., Maillard, P., Poirier, C. (2017b). Effect of
8 plant aggregates on mechanical properties of earth bricks. Journal of Materials in Civil Engineering, 29 (12).
9 [https://doi.org/10.1061/\(ASCE\)MT.1943-5533.0002096](https://doi.org/10.1061/(ASCE)MT.1943-5533.0002096)

10 (Laborel-Préneron et al. 2017c) Laborel-Préneron, A., Magniont, C., Aubert, J.-E., Characterization of Barley Straw, Hemp
11 Shiv and Corn Cob as Resources for Bioaggregate Based Building Materials, Waste Biomass Valor (2018) 9:1095–1112 DOI
12 [10.1007/s12649-017-9895-z](https://doi.org/10.1007/s12649-017-9895-z)

13 (Ramos 2007) Ramos (2007). A importância da inércia higroscópica no comportamento higrotérmico dos edifícios. Faculdade
14 de Engenharia da Universidade do Porto.

15 (AFNOR 2013) AFNOR, “NF V18-122 - Aliments des animaux -Détermination séquentielle des
16 constituants pariétaux - Méthode par traitement aux détergents neutre et acide et à l’acide sulfurique.”
17 2013

18 (Rosario Madrid 2009) Rosario Madrid, M, Estudo das Características Físico-Químicas da Casca de Arroz e Cinzas de Casca
19 de Arroz. Casos de Aplicação. Master Dissertation 2009, IST (in Portuguese)

20 (Ikeagwuani, et al 2019) Ikeagwuani C.C, Nwon D. C., Emerging trends in expansive soil stabilisation: A review, Journal of
21 Rock Mechanics and Geotechnical Engineering, Volume 11, Issue 2, 2019, Pages 423-440,
22 <https://doi.org/10.1016/j.jrmge.2018.08.013>.

23 Faria P, Brás A (2017), Faria P, Brás A (2017), Building physics. Performance of Bio-based Building Materials. D. Jones & C.
24 Brischke (eds.), Woodhead Publishing Series in Civil and Structural Engineering, 335-344.

25 Liuzzi S., Rubino C., Stefanizzi P., Petrella A., Boghetich A., Casavola C., Pappaletta G. (2018) Hygrothermal properties of
26 clayey plasters with olive fibers. Construction and Building Materials 158, 24-32.
27 <https://doi.org/10.1016/j.conbuildmat.2017.10.013>

28

29